Resonant Damping of Helicon Waves in Potassium

A. LIBCHABER* AND C. C. GRIMES
Bell Telephone Laboratories, Murray Hill, New Jersey 07974
(Received 28 August 1968)

A comprehensive experimental study of resonant or collisionless damping of helicon waves has been performed in high-purity potassium. Four different resonant damping effects were studied: cyclotron damping, Landau damping, giant quantum oscillations in the Landau damping, and damping due to helicon–acoustic-wave interaction. All effects were studied under stronger nonlocal conditions than in previous work by employing specimens having electron mean free paths of 0.3 mm and utilizing experimental frequencies up to 170 MHz. An abrupt cyclotron damping edge and giant quantum oscillations were observed for the first time. The observations are in close agreement with predictions based on the free-electron model.

I. INTRODUCTION

THIS paper reports an experimental study of resonant or collisionless damping of helicon waves[1–4] propagating in potassium. Four different resonant damping effects have been studied: cyclotron damping, Landau damping, giant quantum oscillations in the Landau damping, and damping due to interaction of helicon waves with transverse sound waves. This work thus presents a complete study of all the resonant damping mechanisms known to exist in a metal having a spherical Fermi surface.

Resonant damping effects occur only under nonlocal conditions; that is, when the electron mean free path l is larger than the helicon wavelength. Nonlocal conditions prevail when $kl \gg 1$, where k is the helicon wave vector. Values of the dimensionless nonlocal parameter kl as large as 270 have been achieved by employing higher purity potassium and higher frequencies than in previous work. Under such highly nonlocal conditions, giant quantum oscillations in the Landau damping and an abrupt cyclotron damping edge have been observed for the first time. The dimensionless parameter kR (R is the Larmor radius) denotes the short-wavelength ($kR>1$) or long-wavelength ($kR<1$) regions, and plays an important role in delineating the regimes where different damping mechanisms are operative. Improved experimental conditions have permitted extension of studies of Landau damping and helicon-phonon interaction to shorter wavelengths ($kR\sim1$), where resonant effects are most pronounced.

Ordinarily, electromagnetic waves are rapidly damped in metals over distances of the order of the skin depth. However, in the presence of a strong dc magnetic field various modes of wave propagation become possible.[5,6] At low frequencies, i.e., at $\omega<\omega_c$, where $\omega_c=eH/mc$ is the cyclotron frequency of the carriers, a helicon wave can propagate along the dc magnetic field in an uncompensated electron gas. The transverse part of the conductivity tensor determines the propagation character, and for very long wavelengths ($kR\ll1$) collision damping is the main process for wave attenuation. The damping decrement due to collisions is proportional to $(\omega_c\tau)^{-1}$, where τ is the carrier relaxation time. For short wavelengths ($kR\sim1$) resonant damping mechanisms appear. The following paragraphs briefly describe the four mechanisms studied.

Cyclotron damping occurs when moving electrons experience a transverse electric field which rotates at the same rate as do the electrons in their helical motion about the field H. This phenomenon is also called Doppler-shifted cyclotron resonance.[1,7–10] Cyclotron damping is so severe that the wave does not propagate for magnetic fields smaller than a limiting field defined by the condition $kR=1$. Hence, $kR=1$ defines the position of a cyclotron damping edge. A study of the position of the edge in frequency and field provides a direct measurement of the Fermi momentum along the field. The position and shape of the cyclotron damping edge are sensitive to such effects as "Overhauser[11] spin-density waves" and electron-electron correlations.[12]

Landau damping occurs when the helicon wave exerts a longitudinal force on the electrons streaming along the magnetic field in phase with the wave. In potassium this is possible only if $\mathbf{k}$ is not parallel to $\mathbf{H}$.[5,13] (For $\mathbf{k}$ parallel to $\mathbf{H}$ the helicon wave in a free-

* Permanent address: Ecole Normale Supérieure, Paris, France.

[1] O. V. Konstantinov and V. I. Perel, Zh. Eksperim. i Teor. Fiz. **38**, 161 (1960) [English transl.: Soviet Phys.—JETP **11**, 117 (1960)].

[2] P. Aigrain, in *Proceedings of the International Conference on Semiconductor Physics, Prague, 1960* (Academic Press Inc., New York, 1961), p. 224.

[3] R. Bowers, C. Legendy, and F. Rose, Phys. Rev. Letters **7**, 339 (1961).

[4] A. Libchaber and R. Veilex, Phys. Rev. **127**, 774 (1962).

[5] E. A. Kaner and V. G. Skobov, Zh. Eksperim. i Teor. Fiz. **45**, 610 (1963) [English transl.: Soviet Phys.—JETP **18**, 419 (1964)].

[6] E. A. Kaner and V. G. Skobov, Physics **2**, 165 (1966).

[7] P. B. Miller and R. R. Haering, Phys. Rev. **128**, 126 (1962).

[8] E. A. Stern, Phys. Rev. Letters **10**, 91 (1963).

[9] P. M. Platzman and S. J. Buchsbaum, Phys. Rev. **132**, 2 (1963).

[10] J. Kirsch and P. B. Miller, Phys. Rev. Letters **9**, 421 (1962); J. Kirsch, Phys. Rev. **133**, A1390 (1964).

[11] A. W. Overhauser, Phys. Rev. Letters **13**, 190 (1964); A. W. Overhauser and A. M. de Graaf, Phys. Rev. **168**, 763 (1968).

[12] P. M. Platzman and K. C. Jacobs, Phys. Rev. **134**, A974 (1964).

[13] S. J. Buchsbaum and P. M. Platzman, Phys. Rev. **154**, 395 (1967).

electron gas has a purely transverse polarization and cannot impart longitudinal energy to the electrons.) Landau damping arises from the force exerted on the electrons through the interaction of their orbital magnetic moments with the gradient of the longitudinal magnetic field. This force is proportional to kR so the Landau damping becomes unimportant in the long-wavelength limit where $kR \ll 1$.

In the quantum regime, $\hbar\omega_c > k_B T$, quantization of the electron orbits affects cyclotron and Landau damping. When Landau level quantization occurs, the resonant damping mechanisms are inoperative at certain values of the applied magnetic field because the final states for electron transitions are already occupied. Thus oscillations of Landau and cyclotron damping as a function of the magnetic field should be observed and are referred to as giant quantum oscillations.[14–17] The periods of the oscillations are related to the de Haas–van Alphen period, and the amplitudes of the oscillations are much larger than the Schubnikov–de Haas oscillations in magnetoresistance.

The last resonant interaction which leads to collisionless damping of the helicon wave is the helicon-sound wave interaction[18–22] (helicon-phonon interaction in the quantum picture). The helicon wave phase velocity can, in potassium, easily equal a transverse sound velocity. When the phase velocities are equal the two waves interact through inductive coupling and the interaction feeds energy from the helicon wave to the sound wave thereby damping the helicon wave.

The organization of the remainder of the paper is as follows: Sec. II outlines the theory of helicon-wave propagation and presents the theoretical expressions needed to interpret our experimental results; it contains nothing that is original. Section III contains a brief description of our experimental technique. Section IV reports an experimental study of cyclotron damping. We find an abrupt damping edge. Its position is in better agreement with the free-electron gas model than with Overhauser's predicted spin-density-wave gound state for potassium. Section V presents a study of Landau damping. We find that up to very near $kR = 1$ the damping follows Kaner and Skobov's theory[5] although that theory is in principle valid only for $kR < 1$. In Sec. VI we show the first experimental evidence for the existence of giant quantum oscillations in Landau damping. Section VII is devoted to a study of the helicon-sound wave interaction. An attenuation of the helicon wave appears at the field where the wave velocities are matched. The nonlocal effects predicted by Quinn and Rodriguez[21] and Skobov and Kaner[19] are observed. Section VIII contains a brief summary and the conclusions drawn from this work.

II. THEORY

In this section we outline the derivation of the infinite medium helicon wave dispersion relation for a medium having a spherical Fermi surface. This dispersion relation is compared with our experimental results in Secs. IV–VII. Konstantinov and Perel[1] first derived the helicon wave dispersion relation for a metallic medium. Here we follow the more complete derivation presented by Kaner and Skobov.[5]

Consider an infinite medium consisting of n electrons per unit volume neutralized by a uniform, rigid positively charged background. The propagation of plane monochromatic waves is determined by Maxwell's equations and the constitutive equation for the medium

$$k^2\mathbf{E} - \mathbf{k}(\mathbf{k}\cdot\mathbf{E}) = (4\pi i\omega/c^2)\mathbf{j}, \tag{1}$$

$$\mathbf{j}_\alpha = \sigma_{\alpha\beta}(\mathbf{k},\omega,\mathbf{H})E_\beta. \tag{2}$$

We neglect the displacement current, i.e., $\mathbf{k}\cdot\mathbf{j}=0$, which is equivalent to the condition of no space charge in the metal. We choose an $x\eta\zeta$ coordinate system with $\zeta \| k$ and x perpendicular to $\mathbf{H}$ and $\mathbf{k}$. The angle between $\mathbf{H}$ and $\mathbf{k}$ is denoted by φ.

The longitudinal component of the electric field E_ζ taken from Eq. (2) and replaced in Eq. (1) gives

$$(\delta_{\alpha\beta} - 4\pi i\omega k^{-2}c^{-2}\tilde{\sigma}_{\alpha\beta})E_\beta = 0, \quad \alpha,\beta = x,\eta \tag{3}$$

for the plane transverse to $\mathbf{k}$, where

$$\tilde{\sigma}_{\alpha\beta} = \sigma_{\alpha\beta} - \sigma_{\alpha\zeta}\sigma_{\zeta\beta}/\sigma_{\zeta\zeta}.$$

The dispersion relation is obtained by equating to zero the determinant of the coefficients of E in Eq. (3). The dependence of $\sigma_{\alpha\beta}$ on $\mathbf{k}$, ω, $\mathbf{H}$ is complicated; to obtain the dispersion equation asymptotic expressions for $\sigma_{\alpha\beta}$ have to be used. In the two limiting cases $kR \gg 1$ and $kR \ll 1$ the asymptotic expressions for σ are readily calculated. The regime $kR \ll 1$ is the one where lightly damped helicon waves can propagate. In this regime Kaner and Skobov find for $\omega \ll \nu \ll \omega_c$, where $\nu = 1/\tau$ is the collision frequency,

$$\tilde{\sigma}_{\alpha\beta} = \frac{nec}{H\cos\varphi}\begin{bmatrix} \dfrac{\cos\varphi}{\omega_c\tau} + \dfrac{3\pi}{8}kR\sin^2\varphi & -1 \\ +1 & \dfrac{1}{\omega_c\tau\cos\varphi} \end{bmatrix} \tag{4}$$

[14] V. G. Skobov and E. A. Kaner, Zh. Eksperim. i Teor. Fiz. **46**, 1809 (1964) [English transl.: Soviet Phys.—JETP **19**, 1219 (1964)].

[15] P. B. Miller, Phys. Rev. Letters **11**, 537 (1963).

[16] J. J. Quinn, Phys. Letters **7**, 235 (1963).

[17] A. J. Glick and E. Callen, Phys. Rev. **169**, 530 (1968).

[18] G. Akramov, Fiz. Tverd. Tela **5**, 1310 (1963) [English transl.: Soviet Phys.—Solid State **5**, 955 (1963)].

[19] V. G. Skobov and E. A. Kaner, Zh. Eksperim. i Teor. Fiz. **46**, 273 (1964) [English transl.: Soviet Phys.—JETP **19**, 189 (1964)].

[20] D. N. Langenberg and J. Bok, Phys. Rev. Letters **11**, 549 (1963).

[21] J. J. Quinn and S. Rodriguez, Phys. Rev. Letters **11**, 552 (1963); Phys. Rev. **133**, A1589 (1964).

[22] C. C. Grimes and S. J. Buchsbaum, Phys. Rev. Letters **12**, 357 (1964).

and the helicon wave dispersion relation becomes

$$k^2=\omega_p^2\omega\left\{\omega_c c^2\cos\varphi\left[1-i\left(\frac{1}{\omega_c\tau}+\frac{3\pi}{16}kR\sin^2\varphi\right)\right]\right\}^{-1}, \quad (5)$$

where $\omega_p^2=4\pi ne^2/m$. A second coordinate system is denoted by xyz, where $\mathbf{H}\|\hat{z}$. Then the polarization is such that $E_y=iE_x/\cos\varphi$, $E_z=0$. For propagation along the magnetic field ($\varphi=0$)

$$k^2=\omega_p^2\omega[\omega_c c^2(1-i/\omega_c\tau)]^{-1},\qquad E_y=iE_x,\quad E_z=0, \quad (6)$$

these are helicon waves which are circularly polarized and damped only by electron collisions (damping decrement $\propto 1/\omega_c\tau$).

When the helicon wave propagates at an angle to the magnetic field, the wave-phase velocity is reduced by $\cos^{1/2}\varphi$, the wave becomes elliptically polarized, and a collisionless damping mechanism, Landau damping, appears. The Landau damping introduces the additional damping term $(3\pi/16)kR\sin^2\varphi$ in Eq. (5).

To obtain an expression for σ which is valid as $kR\to 1$ we follow Miller and Haering.[7] When $\varphi=0$ the circularly polarized Fourier components of the conductivity are

$$\sigma_\pm=\sigma_0\tfrac{3}{4}\int_0^\pi\frac{d\theta\sin^3\theta}{1-i\tau(\omega\pm\omega_c-kv_F\cos\theta)}, \quad (7)$$

where σ_0 is the dc conductivity $ne^2\tau/m$ and v_F is the Fermi velocity. The integral in (7) can be expressed in closed form. The dispersion relation is obtained by substituting (7) into (3) and equating the coefficients of E to zero. Using σ_-, the dispersion relation becomes

$$k^2=\frac{\omega_p^2}{c^2}\frac{\omega}{\omega_c}\frac{3}{4kR}\left[(1-\gamma^2)\ln\left(\frac{\gamma+1}{\gamma-1}\right)+2\gamma\right]\approx\frac{\omega_p^2\omega}{c^2\omega_c}f(kR), \quad (8)$$

where $\gamma=(\omega_c-\omega+i/\tau)/kv_F\approx 1/kR$. Note that when $kR<1$ then $\gamma>1$ and the argument of the logarithm in (8) is essentially positive which yields a real positive value of k^2. Conversely, when $kR>1$ then $\gamma<1$ and the argument of the logarithm is basically negative. This produces a complex value of k^2 which indicates that the wave is severely damped. Hence, $kR=1$ defines the position of a damping edge. The abruptness of the onset of damping at the edge is determined by the electron mean free path. The mechanism responsible for the cyclotron damping edge is well known to be Doppler-shifted cyclotron resonance. Cyclotron damping also contributes to the dispersion of the wave. As $kR\to 1$ from below, $f(kR)\to\frac{3}{2}$, which indicates that the wave-phase velocity is decreased as the cyclotron damping edge is approached. For a more detailed discussion of the evolution of the real and imaginary parts of k near the edge, see the accompanying paper by Baraff.[23]

III. EXPERIMENTAL METHODS

The experimental configuration which we have employed at frequencies up to 200 MHz to transmit helicon waves through thin slab-shaped specimens (0.2×8×8 mm) is similar to that of Grimes and Buchsbaum.[22] For this configuration a receiver and a transmitter coil are placed at opposite faces of the specimen. The coils consist of a few turns (2 turns at the highest frequency) of No. 40 copper wire wound on a form which has a rectangular cross section. Each coil is imbedded in epoxy in a square opening in one face of a brass housing. The face of each housing is lapped until it is flat and the turns of the coil are recessed back from the face by only ≈0.02 mm. When a specimen is mounted between the two coils and rf current is passed through the transmitter coil, eddy currents are induced at the surface of the specimen due to the *near field* pattern of the coil. The launching wave is thus a linearly polarized plane wave that propagates perpendicular to the surface of the specimen. At the opposite face a part of the transmitted energy is coupled to the receiver coil and fed to a continuously tuneable phase-sensitive detector,[24] which derives its phase reference from the transmitter. The output of the phase-sensitive detector is displayed on an X-Y recorder as a function of the applied magnetic field. The displayed signal is then an interference pattern (Fig. 1) as the transmitted signal becomes alternately in and out of phase with the reference signal. The interference technique was used in the majority of our work; however a second technique which yields a vector representation (phase-amplitude plot) of the transmitted signal was also developed and is briefly described in the Appendix. The major difficulty in trying to apply the interference technique at even higher frequencies is caused by the leakage signal becoming too large. The leakage signal is due to spurious coupling of the transmitter to the receiver. To reduce stray capacitive coupling the sample should be grounded to the brass coil housings which serve as rf shields.[25] Our potassium specimens are covered with sheets of Mylar to retard oxidation of the potassium so we were unable to ground the specimens. (This technique has been used at frequencies up to 4 Gc/sec in a study of Alfven waves in bismuth specimens which were grounded.)

[23] G. A. Baraff, following paper, Phys. Rev. 178, 1155 (1969).

[24] J. W. Hansen, C. C. Grimes, and A. Libchaber, Rev. Sci. Instr. 38, 895 (1967).

[25] In more recent work we have succeeded in grounding the potassium specimen by covering only its center portion with Mylar and covering its rim with a clean gold foil in good electrical contact with the potassium. Using this technique, −120-dB isolation between transmitter and receiver has been achieved [A. Libchaber and C. C. Grimes (to be published)].

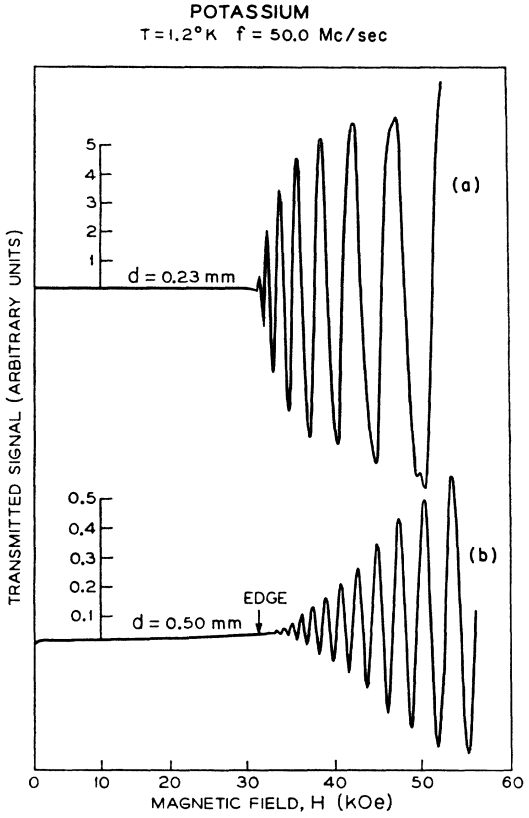

FIG. 1. Two examples of cyclotron damping edge observed by transmission technique. At fields below the edge ($H<31.7$ kOe) there is no wave transmission due to severe cyclotron damping. As the field increases there is an onset of wave propagation at the edge and the interference pattern characteristic of the propagating helicon wave appears for still higher fields.

In the Landau damping experiments the specimen and coils are rotated to various orientations relative to the applied field. Note that if the excitation is uniform over the specimen face, the wave will propagate perpendicular to that face regardless of the direction of the magnetic field.

The specimens are prepared by pressing high-purity potassium slabs covered with mineral oil between two Mylar sheets. The resulting specimen is a polycrystal whose single crystal grains are typically ≈ 1 mm^2 in area. The electron mean free path is ≈ 0.3 mm at 1.5°K. The specimens used ranged in thickness from 0.06 to 0.50 mm.

IV. CYCLOTRON DAMPING

Cyclotron damping of the helicon wave occurs when electrons moving relative to the wave see a wave whose apparent frequency $\omega_D=\omega-\mathbf{k}\cdot\mathbf{v}$ has been Doppler-shifted to the cyclotron frequency ω_c. The moving electrons then undergo cyclotron resonance which transfers energy from the wave to the electrons and damps the wave. Typical numerical values encountered in our experiments are $\omega\approx 10^8 s^{-1}$, $k\approx 10^4$ cm^{-1}, and $v_F\approx 10^8$ cm/sec. Thus when $\mathbf{k}$ and $\mathbf{v}$ are antiparallel, the Doppler shift is positive and much larger than the wave frequency. For $\omega\ll\omega_c$ cyclotron damping occurs whenever the condition $\mathbf{k}\cdot\mathbf{v}=\omega_c$ is satisfied by some group of electrons. In potassium the Fermi surface is essentially spherical so there are some electrons moving along k at all speeds from $-v_F$ to $+v_F$, where $\mathbf{v}_F$ is the Fermi velocity. Consequently, cyclotron damping occurs for all magnetic fields such that $kv_F>\omega_c$, which is equivalent to $kR>1$ for a spherical Fermi surface. Hence, this form of damping occurs at all magnetic fields below the cyclotron damping edge at $kR=1$. In the simple local dispersion relation, Eq. (6), $k\propto(\omega/H)^{1/2}$, which leads to $\omega\propto H^3$ at the cyclotron damping edge; furthermore, the same proportionality is found to hold in the detailed nonlocal theory, Eq. (8).

Experimental studies of cyclotron damping of helicon waves have been performed by Taylor, Merrill, and Bowers[26] using standing wave techniques, by Taylor[27] using surface impedance measurements, and by several workers using variations of the transmission technique described in Sec. III.[27–29] In all previous experiments employing the transmission technique relatively thick or impure specimens were used and the cyclotron damping edge was quite smeared out as in Fig. 1(b). Such data do not yield a precise measurement of the position of the edge. In our studies of cyclotron damping, we used thin specimens (≈ 0.2 mm thick) of high-purity potassium[30] (residual resistivity ratio=13 000). The onset of cyclotron damping is found to be very abrupt, as shown in Fig. 1(a). These are the first transmission data that allow a precise determination of the position of the cyclotron damping edge.

An abrupt cyclotron damping edge was predicted by Platzman and Buchsbaum[9] in their calculation of helicon wave transmission through a plasma slab. They assumed specular reflection of the electrons at the surfaces of the slab, and they used numerical parameters in their computations that are not appropriate for comparison with our experiments. Recently Baraff[23] has performed more realistic calculations in which he treats both the diffuse and specular scattering assumptions and he considers electron mean free paths both greater than and less than the thickness of the slab. Baraff finds that, in principle, one can determine the electron mean free path and whether the scattering is predominantly specular or diffuse by studying the

[26] M. T. Taylor, J. R. Merrill, and R. Bowers, Phys. Letters **6**, 159 (1963).

[27] M. T. Taylor, Phys. Rev. Letters **12**, 497 (1964); Phys. Rev. **137**, 1145 (1965). In these papers several different criteria such as the maximum in $\mathfrak{R}(H)$, the midpoint of $d\mathfrak{R}/dH$, and the minimum in $d\mathfrak{X}/dH$ were used to operationally define the position of the damping edge (here $\mathfrak{R}$ and $\mathfrak{X}$ are the real and imaginary parts of the surface impedance). Calculations (Refs. 31 and 32) have shown that these criteria can differ appreciably from our criterion, $kR=1$.

[28] C. C. Grimes, *Plasma Effects in Solids* (Dunod Cie., Paris, 1965), p. 87.

[29] J. L. Stanford and E. A. Stern, Phys. Rev. **144**, 534 (1966).

[30] P. H. Schmidt (to be published).

amplitude of the transmitted helicon wave very near the damping edge. In the accompanying paper, Baraff compares some of our transmission data with his calculated transmission curves.

By repeating measurements of the cyclotron damping edge at many different experimental frequencies, the theory of cyclotron damping can be tested over a wide range of the nonlocal parameter kl. In Fig. 2 we show a plot of ω versus H at the cyclotron damping edge. The experimental data points were obtained from curves similar to Fig. 1(a) by noting the field where the envelope of the interference pattern extrapolates to zero transmitted amplitude, i.e., the field for onset of a transmitted signal. The solid curve in Fig. 2 is a plot of ω versus H, where $kR=1$ according to Eq. (8), assuming $\tau \rightarrow \infty$.

In Fig. 2 the experimental data points fall consistently at lower fields than the line $kR=1$. In the field interval 10–20 kOe our data points lie $\approx 2\frac{1}{2}\%$ lower in field than $kR=1$ and agree within experimental error with Taylor's measurements. In the magnetic field interval from 30–40 kOe the data points lie $\approx 1\%$ low in field and the discrepancy increases to about 2% for fields from 40–48 kOe. At the higher magnetic fields employed in our experiment, ≈ 48 kOe, the nonlocal parameter becomes $kl \approx 270$. In this case the correction that would be introduced by using the actual collision time τ in Eq. (8) is negligible compared to our experimental uncertainty of $\pm 1\%$ in field.

Baraff's calculations for a free-electron model indicate that the observed edge should lie slightly to the low-field side of $kR=1$ because the onset of damping is not infinitely sharp. For example, in Baraff's Fig. 6 the onset of propagation is calculated to occur below $kR=1$ by $\approx 0.7\%$ for diffuse scattering or $\approx 1.7\%$ for specular scattering of the electrons at the surfaces of the specimen.

A detailed comparison of the predicted and observed position of the edge is of interest to test Overhauser's proposed spin-density-wave (SDW) or charge-density-wave (CDW) ground-state model for potassium.[11] In these models the electronic ground state of potassium possesses either a SDW or a CDW. Either of these waves modifies the electron energy spectrum and distorts the Fermi surface. The Fermi surface becomes "lemon shaped" with the symmetry axis parallel to the wave vector $\mathbf{Q}$ of the SDW or CDW. Since such a distortion has not appeared in de Haas–van Alphen or cyclotron resonance experiments, Overhauser has hypothesized that $\mathbf{Q}$ orients preferentially parallel to the applied field. In this case the extremal cross section of the Fermi surface in a plane perpendicular to $\mathbf{H}$ is still a circle, but with an area slightly smaller than that of the free-electron model. Hence, if $\mathbf{Q}$ orients parallel to $\mathbf{H}$ the results of de Haas–van Alphen and cyclotron resonance experiments will differ very little from the free-electron model. However, the position of the cyclotron damping edge depends on the radius of curvature of the Fermi surface in the direction parallel to $\mathbf{H}$ (assuming $\mathbf{k}\|\mathbf{H}$). If $\mathbf{Q}$ is parallel to $\mathbf{H}$ then calculations predict that in a surface impedance measurement the edge will appear $\approx 4\%$ lower in field than the point $kR=1$ in the free-electron gas model.[31,32] Assuming that the edge would be shifted the same amount in a transmission experiment, then our high-field results would differ from the SDW and CDW models by $\approx 2\%$, whereas they agree within experimental uncertainty with Baraff's calculations for a free-electron gas.

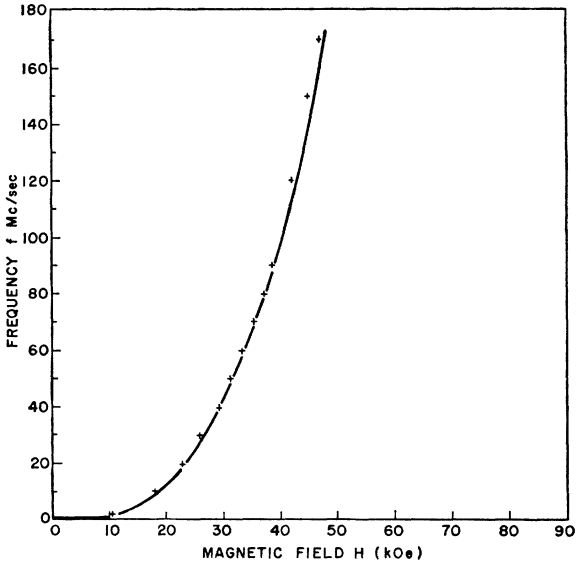

FIG. 2. The crosses represent the frequencies and fields where the cyclotron damping edge was observed in potassium. The solid line represents the theoretically predicted position of the edge.

Platzman and Jacobs[12] have calculated how electron-electron interactions will affect the cyclotron damping edge. They find that the interactions will have observable consequences only if $\omega \approx \omega_c$ in contrast to our experimental conditions where $\omega \ll \omega_c$. Unreasonably large magnetic fields are required to fulfill their condition $kv_F/\omega \approx 1$.

V. LANDAU DAMPING

At magnetic fields greater than the cyclotron damping edge where $kR<1$ a new form of collisionless damping called Landau damping appears when the helicon wave propagates at an angle to the magnetic field. In this field regime there are no electrons moving fast enough to experience Doppler-shifted cyclotron resonance. Instead, Landau damping arises when some moving electrons experience helicon wave fields having a Doppler-shifted frequency equal to zero. The moving electrons then move in phase with the helicon wave

[31] A. W. Overhauser and S. Rodriquez, Phys. Rev. 141, 431 (1966).

[32] J. C. McGroddy, J. L. Stanford, and E. A. Stern, Phys. Rev. 141, 437 (1966).

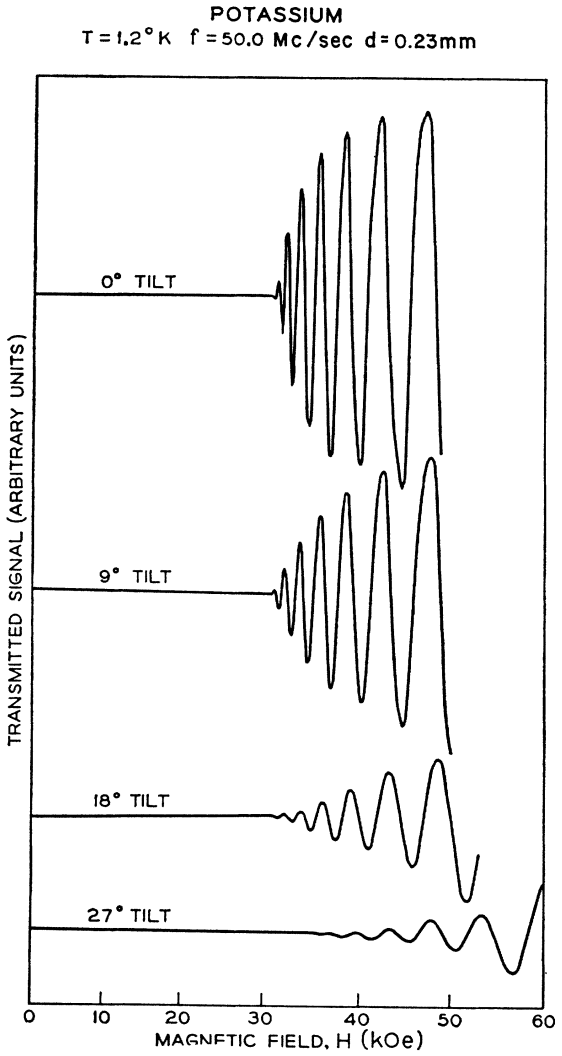

FIG. 3. Series of traces showing how Landau damping attenuates the transmitted signal as the angle between the field and the propagation direction increases.

and can very effectively extract energy from the component of the wave field which is parallel to **H**.

Buchsbaum and Platzman[13] have extended the derivation first given by Kaner and Skobov[5] and have emphasized what physical effects occur in Landau damping. They pointed out that two forces act on the electrons moving in phase with the wave in Landau damping: a magnetic force due to the gradient in H_z and an electric force due to the longitudinal electric field E_z ($\hat{z}$ denotes the direction of the static magnetic field). In a free-electron gas both of these forces vanish when the helicon wave propagates parallel to the static magnetic field. The magnetic force on the drifting electrons has the form $\mu(\partial H_z/\partial z)$, where $\mu=\frac{1}{2}mv_\perp^2/H$ is the orbital magnetic moment of the electron. This force can be described as arising from the moving magnetic mirrors formed by the vector sum of the helicon wave and static magnetic fields. The electric force eE_z simply arises from the small longitudinal component of the helicon wave electric field. Since potassium represents a very low impedance medium, the helicon-wave electric field is much smaller than the wave magnetic field. Buchsbaum and Platzman have shown that the ratio of the electric force to the magnetic force is $v_H/v_F\approx 10^{-3}$, where v_H is the helicon phase velocity and v_F the Fermi velocity.

The first experimental study of Landau damping of helicon waves was performed by Walpole and McWhorter[33] at microwave frequencies in n-type PbTe. Landau damping experiments on potassium were first reported by Grimes and Libchaber,[34] who employed the transmission technique of Sec. III. Subsequently, Houck and Bowers[35] have reported Landau damping studies on Na and K using both standing wave and transmission techniques. The work of Houck and Bowers is reasonably detailed and complete, so we will present here only a brief summary of our results at higher frequencies using thin specimens of higher purity whereby larger values of the nonlocal parameter kl are achieved and larger values of kR are studied.

Landau damping is observed by the transmission method described in Sec. III. Experimental curves illustrating Landau damping at different tilt angles (different angles between **k** and **H**) are shown in Fig. 3. The increase in damping as the tilt angle increases is seen to be most severe near the cyclotron damping edge, i.e., near $kR=1$.

To compare theory and experiment, we measure the amplitudes $A(\varphi)$ and $A(0)$ of the helicon waves transmitted at a given value of k for a finite tilt angle and for zero tilt angle. We then plot $\ln[A(0)/A(\varphi)]=\Delta$ versus kR, where k is the wave vector calculated from Eq. (8) corrected for finite φ. Assuming the wave varies as $\exp i(k_r+ik_i)z$ and assuming $k_r\gg k_i$ then from Eq. (5) we have $\ln[A(0)/A(\varphi)]=(3\pi/32)kR\sin^2\varphi$. Hence theory predicts that our plot will be a straight line of slope $(3\pi/32)\sin^2\varphi$. In Fig. 4 we have plotted the data points from the $\varphi=18°$ tilt curve of Fig. 3 and we have drawn the line predicted by Eq. (5). Note that no adjustable parameters have been employed in this comparison of theory and experiment. It is evident that the theory accounts well for the Landau damping at small kR where the assumptions underlying the theory are valid. As kR approaches unity the theory is no longer applicable, but the same straight line agrees surprisingly well with experiment. We would like to emphasize that in this test of the nonlocal theory the nonlocal parameter kl reaches a value of 180, which is a factor of 6 greater than in previous work.

[33] J. N. Walpole and A. L. McWhorter, Phys. Rev. **158**, 708 (1967).
[34] C. C. Grimes and A. Libchaber, Bull. Am. Phys. Soc. **12**, 771 (1967).
[35] J. R. Houck and R. Bowers, Phys. Rev. **166**, 397 (1968).

VI. GIANT QUANTUM OSCILLATIONS

Quantum effects in helicon wave propagation become significant at high magnetic fields and low temperatures ($\hbar\omega_c > k_BT$) where the electron energy states are quantized into Landau levels. The most common manifestations of quantum effects are small oscillations of the damping of the wave due to oscillations of the electron relaxation time as the magnetic field is varied. These effects, called ordinary quantum oscillations, are similar to the Shubnikov–de Haas oscillations of magnetoresistance and have been observed by several workers.[36] The ordinary quantum oscillations in metals typically correspond to variations in k_i of only a few percent. Since this paper concerns nonlocal or resonant damping mechanisms, we consider the effects of Landau quantization on Landau and cyclotron damping. Below we show that simultaneous application of the Pauli exclusion principle, conservation of energy, and conservation of momentum results in resonant damping at discrete values of the magnetic field, i.e., as the magnetic field is varied the resonant damping is allowed for only a fraction of each de Haas–van Alphen period. This turning on and off of the resonant damping leads to large fractional oscillations in k_i; hence Gurevich *et al.*[37] termed this dramatic effect "giant quantum oscillations" (GQO).

Let us consider the GQO in Landau damping for an isotropic material. The first treatment of this problem was by Gurevich *et al.* for the case of longitudinal acoustic waves propagating parallel to an applied magnetic field. In a quantizing magnetic field the electron energy states are given by

$$E = p_z^2/2m + (n+\tfrac{1}{2})\hbar\omega_c.$$

Conservation of energy in an intra-Landau level transition requires $\hbar\omega = p_{z2}^2/2m - p_{z1}^2/2m$ and conservation of momentum requires $\hbar k = p_{z2} - p_{z1}$ when a helicon wave photon of frequency ω and wave vector k is absorbed. Combined, these conditions require $p_{z1} = m\omega/k - \frac{1}{2}k$, which means that before the transition the electrons that damp the wave move slightly slower than the wave phase velocity. The Pauli exclusion principle requires that the state of momentum p_{z1} must be occupied and the state of momentum p_{z2} must be unoccupied if photon absorption is to occur. Thus, the Fermi level must lie between these two states which are separated in energy by $\hbar\omega$. Consequently, absorption of photons (Landau damping) occurs over only a fraction ω/ω_c of each de Haas–van Alphen period. Collisions introduce a spread in momentum $\Delta p_z \approx m/k\tau$ of those electrons that remain in phase with the wave over their whole mean free path. For GQO to occur, Δp_z must be smaller than the difference

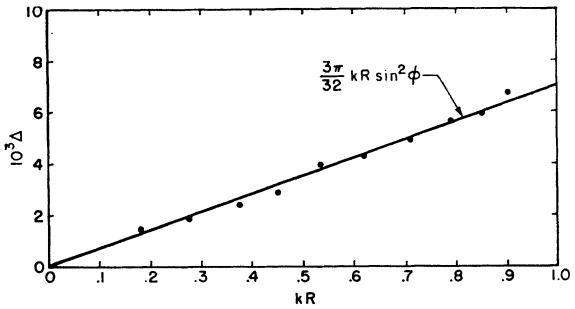

FIG. 4. Comparison of observed and predicted contribution to the imaginary part of the helicon wave vector due to Landau damping for an 18° tilt angle.

in Fermi momenta on two successive Landau levels. This condition requires $(2m\hbar\omega_c)^{1/2} > m/k\tau$ or

$$kl(\omega_c/E_F)^{1/2} > 1. \tag{9}$$

The discussion above follows the treatment of Gurevich *et al.* Skobov and Kaner have presented a similar treatment for helicon waves.[14] Since helicon waves are transverse waves there is no Landau damping in an isotropic material unless the wave propagates at an angle to the magnetic field. Skobov and Kaner find that GQO should appear in the Landau damping of helicon waves provided the following conditions are satisfied:

$$\hbar\omega_c \gg k_BT, \tag{10}$$

$$kR \ll 1, \tag{11}$$

$$\hbar\omega_p^2/mc^2\nu > 1 + \nu/\omega. \tag{12}$$

Condition (12) is equivalent to (9) when the helicon wave dispersion relation (6) is used to express k in terms of ω and H.

Our experimental conditions are characterized by the following quantities: $H \approx 10^5$ Oe, $T \approx 1.2$°K, $\omega \approx 1.2 \times 10^8$ sec^{-1}, $\nu \approx 2.5 \times 10^9$ sec^{-1}, $\omega_p^2/c^2 \approx 4 \times 10^{10}$ cm^{-2}. We find that conditions (10) and (11) are well satisfied. The inequality in condition (12) is not quite satisfied; instead the right and left sides are very nearly equal. At higher experimental frequencies condition (12) is satisfied, but the data at higher frequencies are often more complicated due to the helicon-sound wave interaction.

Note added in proof. In a recent article [E. A. Kaner and V. G. Skobov, Advan. Phys. **17**, 605 (1968)] Kaner and Skobov have shown that the left-hand side of inequality (12) should be multiplied by the quantity $\hbar\omega_c/k_BT$ which has the value 9.1 under our experimental conditions. With this modification inequality (12) is well satisfied.

Our experimental results shown in Fig. 5 represent the first observation of GQO of Landau damping for an electromagnetic wave. In Fig. 5 the angle between the propagation direction and the field direction is 30°. At fields above 90 kOe there appear large quantum oscillations in the amplitude of the transmitted wave.

[36] J. R. Merrill, Phys. Rev. **166**, 716 (1968).
[37] V. L. Gurevich, V. G. Skobov, and Yu. A. Firsov, Zh. Eksperim. i Teor. Fiz. **40**, 786 (1961) [English transl.: Soviet Phys.—JETP **13**, 552 (1961)].

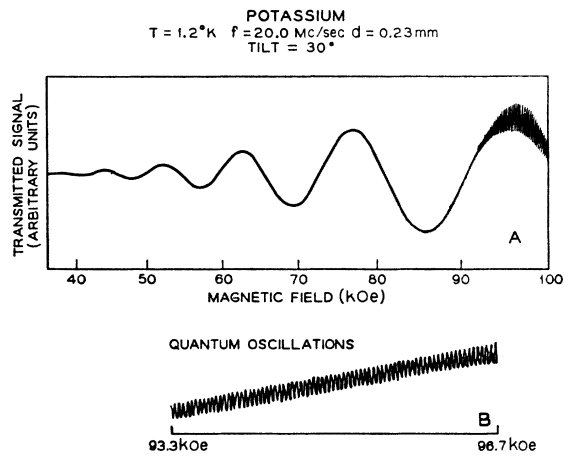

FIG. 5. Experimental traces showing giant quantum oscillations in Landau damping.

Examination of Fig. 5(a) reveals that near 100 kOe the GQO produce maxima in the value of k_i that are more than a factor of 2 larger than the minima in k_i. Figure 5(b) shows an expanded portion of the high-field region. Within our experimental accuracy ($\approx 1\%$), the GQO period obtained in this specimen of unknown crystal orientation falls within the range of de Haas–van Alphen periods of potassium measured by Shoenberg and Stiles.[38] For wave propagation along the magnetic field the oscillations become ordinary quantum oscillations and are two orders of magnitude smaller in amplitude. The GQO disappear when the temperature is raised to 4.2°K, where condition (10) is not well satisfied. For a frequency less than 1 Mc/sec the GQO disappear as expected since condition (12) is violated. At frequencies higher than 20 Mc/sec, larger GQO than those in Fig. 5 are observed, but the data become quite complicated due to the helicon-sound wave interaction. We attempted in Fig. 5(b) to study the line shape of the GQO, but found that our Bitter solenoid was not stable enough for such a study. Since inequality (12) was not satisfied, collision broadening of the GQO is expected to produce an almost sinusoidal line shape. At higher frequencies and in material with larger l where condition (12) is satisfied, theory predicts that the GQO line shape will become a series of spikes.

Skobov and Kaner[14] and Miller and Kwok[39] have pointed out that GQO in Landau damping of helicon waves can also occur when **k** and **H** are parallel provided the electrons that drift along **H** at the wave velocity execute "tilted orbits" in real space. Tilted orbits arise when the Fermi surface is anisotropic and **H** is not along an axis of threefold or higher symmetry. Since potassium has an isotropic Fermi surface, tilted orbits do not occur; however, aluminum has an anisotropic Fermi surface and our experiments on this material indicate that tilted orbits do give rise to GQO.

The physical origin of GQO in cyclotron damping is very similar to that in Landau damping. In cyclotron damping, however, the electron transition is an inter-Landal level transition and the electron's Landau level quantum number increases by 1 as the helicon photon is absorbed. Conservation of energy and momentum then requires $\hbar\omega = p_{z2}^2/2m + \hbar\omega_c - p_{z1}^2/2m$ and $\hbar k = p_{z2} - p_{z1}$. Combined, these conditions require $p_{z1} = -m(\omega_c - \omega)/k - \frac{1}{2}\hbar k$, which shows that the absorbing electrons "see" a Doppler-shifted frequency very nearly equal to the cyclotron frequency. Again, the state of momentum p_{z1} must be occupied and the state of momentum p_{z2} must be unoccupied if photon absorption is to occur. Since the two states are separated in energy by $\hbar\omega$, absorption occurs only over a fraction ω/ω_c of each de Haas–van Alphen period.

The theory of GQO in cyclotron damping of helicon waves in an isotropic material has been treated by Quinn,[16] Miller,[15] and Glick and Callen.[17] Quinn and Miller both demonstrated that the imaginary part of the dielectric constant ϵ_i should display GQO in the cyclotron damped region ($kR > 1$) provided $\omega_c\tau \gg 1$ and $\hbar\omega_c \gg kT$. They suggested that helicon propagation should be observable at the minima of ϵ_i where cyclotron damping is forbidden. Recently Glick and Callen have presented a more detailed theory in which they also find GQO in ϵ_i, but they further demonstrate that ϵ_r is rapidly varying in the regions where ϵ_i (and the cyclotron damping) is small. Due to the rapid variation of ϵ_r, a wide range of k values will be excited by the driving field rather than launching a single wave of well-defined wavelength. Hence, according to Glick and Callen's analysis, the GQO will not be observable by either our transmission technique or by surface impedance measurements.

We have searched for, but have not found, GQO in cyclotron damping of helicon waves in potassium. We employed the transmission technique at frequencies up to 200 Mc/sec and a surface impedance measurement at 24 Gc/sec. For the transmission experiments the magnetic fields ranged up to 45 kOe in the region $kR > 1$. For the surface impedance measurement the field was swept to 103 kOe. The temperature was held at 1.2°K so the condition $\hbar\omega_c \gg k_B T$ was well satisfied. The electron collision time was $\tau \approx 4 \times 10^{-10}$ sec, so the condition $\omega_c\tau \gg 1$ was also well satisfied. Our failure to observe GQO in cyclotron damping supports Glick and Callen's arguments regarding the observability of the GQO.

VII. DAMPING BY HELICON-PHONON INTERACTION

In Sec. V we described how resonant damping arises when electrons move in phase with the helicon wave; in this section we describe how resonant damping arises

[38] D. Shoenberg and P. J. Stiles, Proc. Roy. Soc. (London) A281, 62 (1964).
[39] P. B. Miller and P. C. Kwok, Phys. Rev. 161, 629 (1967).

when phonons or acoustic waves move in phase with the helicon wave. When $\mathbf{H}=0$ the electromagnetic fields accompanying a transverse acoustic wave are very small because the ion current is very nearly cancelled by the induced electron current. However, for large $\mathbf{H}$ such that $\omega_c\tau\gg1$ the current neutrality breaks down because the induced electron current is then nearly orthogonal to the ion current. Hence in a strong dc magnetic field, the induced electromagnetic fields accompanying a transverse acoustic wave are appreciable, and the acoustic wave couples effectively to a helicon wave. When the phase velocities of a transverse acoustic wave and a helicon wave are matched, a resonant transfer of energy occurs between the two. Resonant transfer of energy out of the helicon wave leads to a sharp increase in its damping.

In a previous experiment the helicon-phonon interaction was studied in a thick crystal of potassium with wave propagation along the [110] axis.[22] In that case the interaction was so strong that two waves of mixed helicon and acoustic character were observed. In the present work we report experiments on thin potassium specimens of unknown crystal orientation. The acoustic wave velocities in these experiments are greater than in the previous experiment; consequently the helicon-phonon coupling is weaker. The weaker coupling causes the helicon-phonon interaction to appear as a sharp increase in the damping of the helicon wave when the helicon phase velocity matches a transverse sound velocity. Figure 6 shows a typical curve obtained by the experimental technique described in Sec. III. Since the helicon phase velocity increases continuously with increasing H, sweeping H is equivalent to sweeping phase velocity. In Fig. 6 the two regions of severe

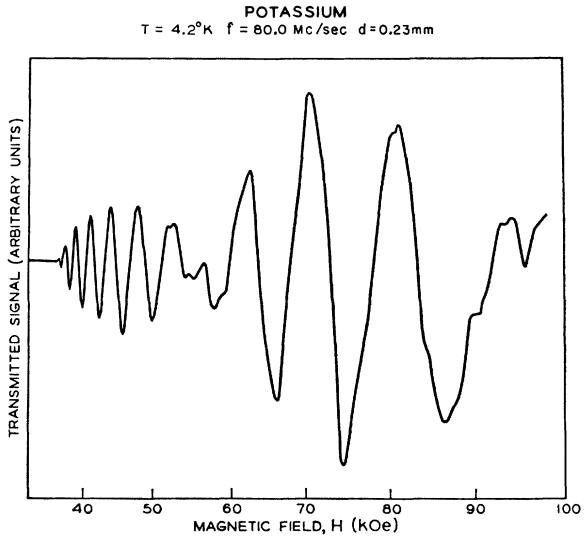

FIG. 6. Experimental trace showing distortion of interference pattern by helicon-phonon interaction. The helicon phase velocity increases with field and matches sound velocities at ≈55 and 95 kOe.

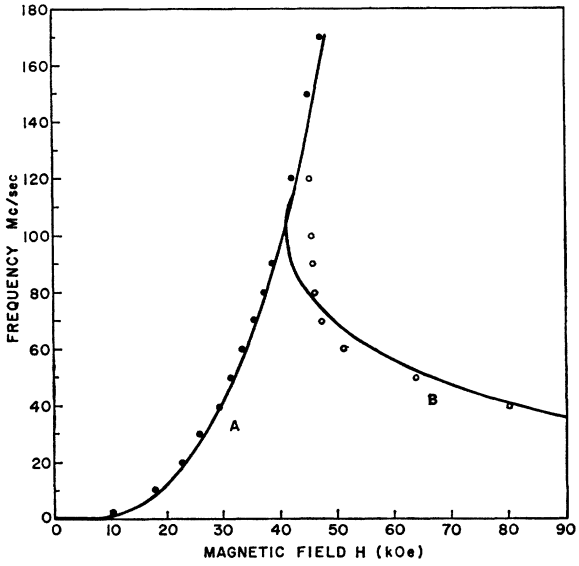

FIG. 7. Curve B and the open circles denote, respectively, the predicted and observed frequencies and fields where the helicon phase velocity matches a sound-wave velocity. Curve A and the solid dots denote the predicted and observed frequencies and fields where the cyclotron damping edge occurs.

damping near 55 and 95 kOe mark the fields where acoustic wave velocities were crossed. The fact that the interaction is well localized in magnetic field allows us to study how cyclotron and Landau damping affect the interaction.

The theory of helicon-phonon interaction has been treated by several authors. The treatments that are most complete and most relevant to our experiments were presented by Skobov and Kaner[19] and Quinn and Rodriguez.[21] The latter work deals with the modification of the interaction when $kR\rightarrow1$ and cyclotron damping becomes important. Skobov and Kaner's treatment includes the deformation potential and the modification of the interaction by Landau damping. Skobov has extended the theory of helicon-phonon interaction to the quantum regime to include GQO in Landau damping.[40] Although we have obtained some data in the quantum regime, we have not attempted to analyze it due to its complexity.

Effects of Cyclotron Damping

By taking a series of experimental traces similar to Fig. 6 at progressively higher helicon wave frequencies, the point of helicon-phonon interaction can be brought progressively nearer the cyclotron damping edge. The results of such a study are shown in Fig. 7. In this figure the open circles denote the frequencies and fields where the interaction occurred, and the solid dots denote the position of the cyclotron damping edge. Curve A represents the equation $kR=1$ while

[40] V. G. Skobov, Fiz. Tverd. Tela 6, 2655 (1964) [English transl.: Soviet Phys.—Solid State 6, 2115 (1965)].

curve B represents the calculated locus of points where the helicon-phase velocity equals a constant. In calculating curve B the nonlocal dispersion relation Eq. (8) was employed and the curve was normalized to the lowest frequency datum point. At frequencies below 70 Mc/sec, where $kR \ll 1$, the point of interaction follows well the curve $v_H = \text{const}$. At higher frequencies $kR \rightarrow 1$ and nonlocal dispersion produces the steep negative slope in curve B near the damping edge. The observed dispersion as $kR \rightarrow 1$ is greater than the calculated dispersion. A more refined calculation including the magnetic field dependence of the velocity of the transverse acoustic wave leads to slightly better agreement between theory and observation, but an unexplained discrepancy remains.

Effects of Landau Damping

When the helicon wave propagates at an angle φ relative to **H**, the strength of the helicon-phonon coupling is reduced by the factor $|\cos\varphi|$ and Landau damping appears. The Landau damping further reduces the helicon-phonon coupling by introducing a spread in the **k** values (Fourier components) describing the spatially decaying helicon wave. We were unable to determine quantitatively the strength of the helicon-phonon coupling in potassium, but we did verify qualitatively that the coupling is reduced significantly as φ is increased from 0 to $\frac{1}{4}\pi$. For a given value of φ, the reduction in coupling is greatest near $kR = 1$, where the Landau damping is most severe.

VIII. SUMMARY AND CONCLUSIONS

Utilizing a transmission technique to observe helicon waves in potassium, we have studied four different resonant damping effects: Landau damping, cyclotron damping, giant quantum oscillations in Landau damping, and helicon-phonon interacting. This work thus presents a fairly complete study of resonant damping mechanisms in a metal having a spherical Fermi surface. Theoretical works based on a free-electron gas model are adequate to account for our observations. Logical extensions of this work would include studies at still higher frequencies in the strong, stable fields now available in superconducting solenoids and studies on higher purity single-crystal specimens. Such studies could provide more explicit tests of the theories of giant quantum oscillations in both Landau damping and cyclotron damping.

ACKNOWLEDGMENTS

We gratefully acknowledge that this work was made possible by P. H. Schmidt's success in purifying the potassium used in the experiments. In the course of this work we have benefited from the technical assistance of G. Adams, H. W. Dail, and J. W. Hansen, and we have profited from stimulating discussions with G. A. Baraff, S. J. Buchsbaum, P. M. Platzman, and P. A. Wolff.

APPENDIX

This appendix outlines an experimental technique that provides a vector representation or phase-amplitude polar plot of the helicon wave signal transmitted through a thin slab-shaped specimen. With this technique both the amplitude and phase of the transmitted signal are displayed as continuous functions of magnetic field on a polar plot as the radius and polar angle, respectively. Such a display has the advantages that all of the information contained in the signal is recorded, and since phase and amplitude are displayed on orthogonal coordinates, the data are unambiguous.

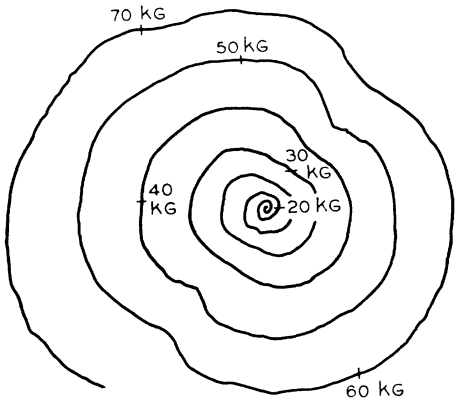

FIG. 8. Phase-amplitude polar plot of the helicon-wave signal transmitted through a potassium slab 0.23 mm thick at a frequency of 10.7 MHz and a temperature of 4.2°K. Distance from center represents amplitude of transmitted signal, while polar angle represents phase delay within specimen.

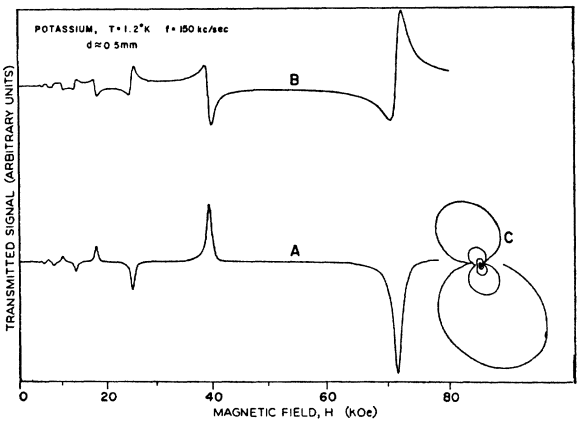

FIG. 9. Curves A and B are experimental traces obtained by the transmission technique for two settings of the reference-signal phase differing by 90°. Curves A and B show, respectively, the amplitude and phase of the third standing-wave resonance at ≈71 kOe, the fourth at ≈40 kOe, etc. Curve C is the phase-amplitude polar plot obtained by plotting A versus B on the ordinate and abscissa, respectively.

The disadvantages of this display are that more equipment is required and the data-taking procedure is more complex, hence slower.

To obtain the phase-amplitude polar plot we use the technique described in Sec. III, but feed the transmitted signal, after amplification, to two lock-in detectors operating in quadrature. The outputs of the lock-ins are to the two axes of an X-Y recorder. The phase references for the two lock-in detectors are derived from the transmitter current—one being in phase and the other 90° out of phase. The details of the high-frequency lock-in detectors used are described by Hansen *et al.*[24]

Experimental traces showing representative phase-amplitude polar plots are shown in Figs. 8 and 9. In Fig. 8 the polar plot appears as a distorted spiral because standing waves within the specimen are becoming significant at the higher magnetic fields. In the absence of standing waves the plot would be an undistorted spiral because the amplitude of the transmitted signal would increase smoothly and the phase delay in the specimen decrease continuously as the applied magnetic field is increased. Standing waves can become quite pronounced when the helicon wavelength is comparable to the specimen thickness as shown in Fig. 9. The polar plot (C) is a spiral at only the lowest fields and evolves into a "figure 8" at the higher fields. Curves (A) and (B) of Fig. 9 show the outputs of the two lock-in detectors which are applied to the X and Y axes, respectively, of the X-Y recorder to generate the polar plot.

PHYSICAL REVIEW VOLUME 178, NUMBER 3 15 FEBRUARY 1969

Transmission of Electromagnetic Waves through a Metallic Slab. III. Effect of Boundary Scattering on Helicon Transmission near Cutoff

G. A. Baraff
Bell Telephone Laboratories, Murray Hill, New Jersey 07974
(Received 28 August 1968)

This paper, like the two in this series which precede it, is concerned with electromagnetic wave propagation under conditions where the relation between the currents in the medium and the electric field driving them is nonlocal because the electron mean free path is comparable to the length over which the fields change. For this case, both the boundary conditions on the electrons reaching the surface of the slab and the more familiar boundary conditions imposed upon the fields are important. Our concern here is the effect of the electronic boundary conditions on helicon wave propagation; in particular, on the way in which Doppler-shifted cyclotron resonance (Dscr) damps the helicon wave as the magnetic field is lowered to the Dscr threshold. Our findings may be summarized briefly as follows: At large magnetic fields, where the helicon wave is relatively undamped and exhibits standing-wave resonances, the assumption of diffuse electronic surface scattering decreases the transmission below the amount calculated assuming specular surface scattering. In addition, it leads to a softening of the resonances (decrease in the standing-wave ratio) relative to the resonances calculated assuming specular electronic surface scattering. This softening decreases as the magnetic field is raised, i.e., as the conductivity becomes local; and in fact, in the local limit, specular and diffuse transmission are identical. As the field is lowered, more of the incident energy goes into the single-particle excitations when the surface scattering is diffuse than when it is specular. Finally, when the field reaches a value close to the Dscr cutoff, the specular calculation exhibits an extra peak absent from the diffuse. The amplitude of this peak, however, is quite low because of its proximity to cutoff. Experimental data are not yet available to determine whether surface scattering is predominantly diffuse or predominantly specular, but the calculations presented here do allow one to determine the mean free path by fitting the shape of the transmission curves near Dscr.

I. INTRODUCTION

RECENT experiments on the transmission of helicon waves[1] through thin slabs of potassium have been reported by Libchaber and Grimes.[2] Among their many findings was the observation that, with the magnetic field normal to the surface of the slab, reducing the field to the Doppler-shifted cyclotron resonance[3] (Dscr) threshold decreased helicon transmission in a way which seemingly depended on the thickness of the slab relative to the mean free path of the electrons in it. In particular, the onset of Dscr appeared to be abrupt when the slab was less than a mean-free-path thick. Slabs whose thickness was greater than a few mean free paths invariably exhibited a transmission decrease

[1] P. Aigrain, in *Proceedings of the International Conference on Semiconductor Physics, Prague, 1960* (Academic Press Inc., New York, 1961), p. 224; R. Bowers, C. Legendy, and F. Rose, Phys. Rev. Letters 7, 339 (1961).

[2] A. Libchaber and C. C. Grimes, preceding paper, Phys. Rev. 178, 1145 (1969).

[3] T. Kjeldaas, Phys. Rev. 113, 1473 (1959).